Third International Symposium on Marine Propulsors
smp'13, Launceston, Tasmania, Australia, May 2013

Numerical simulation of propeller-hull interaction and determination of the effective wake field using a hybrid RANS-BEM approach

Douwe Rijpkema[1], Bram Starke[1], Johan Bosschers[1]

[1]Maritime Research Institute Netherlands (MARIN), Wageningen, The Netherlands

ABSTRACT

In this study propeller-hull interaction is investigated numerically using a combination of a steady viscous CFD method (RANS) for the ship flow and an unsteady potential-flow method (BEM) for the propeller loading. This approach allows for interaction between hull and propeller with a significantly reduced computational effort compared to a full RANS approach. In addition, the RANS-BEM coupling provides the propeller designer with an effective wake field.

RANS-BEM results for self-propulsion are obtained with two different RANS solvers. The computations show a prediction of propeller rotation rate and thrust within 2 to 3% of the experimental values. It is demonstrated that the effective wake accelerates towards the propeller. Therefore the essential part of the RANS-BEM coupling remains how and where to determine the effective wake field. The influence on the propeller performance is shown by evaluating effective wake fields at different planes upstream of the propeller. Extrapolating the effective wake field to the propeller plane using multiple planes upstream results in an increase of about 2 to 3% in predicted rotation rate compared to using a single plane upstream.

Keywords

CFD, RANS-BEM coupling, propeller-hull interaction, effective wake field

1 INTRODUCTION

When a propeller is operating behind a ship the interaction between hull and propeller affects both the resistance of the ship and the loading of the propeller. For an accurate prediction of both it is essential to include this interaction in the design approach. The most obvious and consistent approach to date is simulating both the ship and propeller using a viscous CFD approach. However, this requires large and complex grids around ship and propeller in combination with unsteady simulations, resulting in a large computational effort. In an early design phase, where a first estimate of effective wake field and thrust deduction is desired, a simpler propeller model would suffice. In this study a numerical approach is employed that uses a viscous-flow method (RANS) for the flow around the hull coupled with a potential-flow method (BEM) for the propeller.

Potential-flow methods for propellers are widespread, mature and efficient. These methods can give good predictions of thrust and torque, but are known to produce less accurate results when viscous effects become important, for example in off-design conditions or for highly skewed propellers. For the RANS-BEM approach the BEM propeller loading is transformed to a body force distribution which is imposed in the RANS computation by adding them as source terms to the right-hand-side of the momentum equations, either in a single plane or as a three-dimensional distribution within the swept volume of the propeller.

The inflow to the propeller, required by the BEM, is not the (total) velocity field in the wake of the ship, since the propeller itself induces velocities due to the delivered thrust. It also differs from the nominal wake field (the wake field without propeller action) due to vorticity interaction effects. The resulting inflow wake field for the propeller including the vorticity interaction effects is the so called effective wake. Current practice to determine the effective inflow from model tests is to measure the nominal wake in the propeller plane and to transform it into an effective wake field. Two common approaches to do so are the so-called V-shaped segment method and the force-field method as e.g. described in Carlton (2007). Both methods have limitations in the sense that the propeller-hull interaction is only partially taken into account, and it is only the axial velocity component that is modified. The RANS-BEM coupling provides an alternative way of obtaining the effective wake field by subtracting BEM induced velocities from the RANS computed total wake. This also includes the transverse velocity component and offers the possibility to determine the effective wake directly at full scale Reynolds numbers.

In the next section a description is given of the numerical methods applied in this study. This is followed by an overview of the coupling methodology for the RANS-BEM approach. Results using this approach are presented next for self-propulsion predictions, which are compared with experimental data. In the subsequent part various ways to determine the effective wake field are compared, including

their effect on the propulsive performance predictions. Additionally, a comparison between a RANS-BEM approach and a force-field method is made and differences in the effective wake fields are addressed.

2 NUMERICAL METHODS

The results presented in this paper are obtained using two different RANS solvers: PARNASSOS and ReFRESCO. Both solvers can be coupled with the boundary element method PROCAL. In section 5 a comparison will be made with NOMEFF, a force-field method for predicting the effective wake field. A short description of these methods is presented here.

2.1 PROCAL

For the analysis of the flow past the propeller, use is made of a boundary element method that solves the incompressible potential flow equations for lifting and non-lifting bodies. The method, designated PROCAL, is being developed within MARIN'S Cooperative Research Ships (CRS) for the unsteady analysis of cavitating propellers operating in a prescribed ship wake. It has been validated for open water characteristics, shaft forces and moments, sheet cavitation extents and propeller induced hull-pressure fluctuations. The code is a low order BEM that solves for the velocity disturbance potential. Initial validation studies and details on the mathematical and numerical model can be found in Vaz & Bosschers (2006) and Bosschers et al. (2008). The blade wake can be determined by an iterative procedure to align the geometry of the wake with the flow or by a prescribed wake pitch and contraction using empirical formulations to reduce CPU time. The latter is used for the BEM computations listed in this study. A panel distribution of 60x30 panels was used for the blades in chordwise and radial direction respectively.

2.2 PARNASSOS

PARNASSOS is a viscous-flow code developed and used by MARIN and IST (Hoekstra, 1999; Van der Ploeg et al., 2000). It solves the discretised Reynolds-averaged Navier-Stokes equations for a steady, 3D incompressible flow around a ship's hull. Various eddy-viscosity turbulence models are available. The discretisation is of finite-difference type. All terms in the momentum and continuity equations are discretised by second or third-order accurate difference schemes. PARNASSOS can handle body-fitted, generally non-orthogonal HO-type grids, either single or multi-block structured.

The momentum and continuity equations are solved in fully coupled form and integrated down to the wall. No wall functions are used, not even at full scale. Details about the solution strategy can be found in Van der Ploeg et al. (2000).

For the treatment of the free surface the steady iterative formulation (Van Brummelen et al., 2001; Raven et al., 2004) is used which, contrary to almost all other RANS/FS methods, involves no time-dependent terms; neither in the momentum equations, nor in the free-surface boundary conditions. The problem is solved by an iterative procedure, instead of by time integration (Raven et al., 2004).

For all PARNASSOS simulations presented in this paper a one-equation turbulence model (Menter, 1997) was used, extended with a correction for the longitudinal vorticity (Dacles-Mariani et al., 1995).

2.3 ReFRESCO

ReFRESCO is a MARIN in-house viscous-flow CFD code, spin-off of FreSCo, a code developed together with HSVA and TUHH during the VIRTUE EU project. It solves the multiphase unsteady incompressible RANS equations, complemented with turbulence models and volume-fraction transport equations for different phases. The equations are discretized using a finite-volume approach with cell-centered collocated variables. The implementation is face-based, which permits grids with elements consisting of an arbitrary number of faces (hexahedrals, tetrahedrals, prisms, pyramids, etc.), and h-refinement (hanging-nodes). The code is parallelized using MPI and sub-domain decomposition, and runs on Linux workstations and HPC clusters. The momentum and pressure equations can be solved in a segregated or coupled approach.

The code is targeted at and optimized for hydrodynamic applications. It has already been applied, verified and validated for several flows, in particular for current and manoeuvring coefficients of submarines and ships, cavitating flows and propellers (Vaz et al., 2010; Hoekstra & Vaz, 2009; Rijpkema & Vaz, 2011).

The ReFRESCO simulations in this study have been performed with a second order QUICK discretization scheme for the convective part of the momentum equations. The turbulence model for the simulations is the $k-\omega$ SST model. No wall functions are applied.

2.4 NOMEFF

A traditional approach for correcting the nominal wake field is using a force-field method which uses as input only the nominal wake field in the propeller plane and the propeller thrust loading coefficient. The method has been developed by MARIN for CRS in the 1980's and implemented in the computer code designated NOMEFF. It is assumed that there exists only an axial velocity component in the nominal wake field of which the derivative in axial direction is neglected. The mathematical basis is the Euler equations with an axisymmetric propeller loading included as a force field, varying in radial direction (Van Gent, 1986). The velocities in the Euler equations are decomposed into the axial velocity of the nominal wake and disturbance velocities. After some mathematical manipulations, a set of non-linear equations arises for the disturbance velocities with prescribed force field which can be solved iteratively. The disturbance velocities consist of

the induction velocities of the propeller and the interaction velocities. The induction velocities are obtained from the applied loading distribution using vortex cylinder theory in uniform flow. Subtracting these induction velocities from the disturbance velocity gives the interaction velocity (in axial direction only). Addition of the interaction velocity to the nominal wake field then gives the effective wake field.

3 RANS-BEM COUPLING METHODOLOGY

The coupling between BEM and RANS is performed using an iterative coupling between the velocity fields from both RANS and BEM computations and the force distribution on the propeller blades that follows from the BEM results.

3.1 Coupling procedure

The coupling procedure for RANS-BEM is as follows:

1. First a steady RANS computation is performed without propeller action and the resulting nominal wake field is evaluated at the location of the propeller plane. The nominal wake field is used for the first BEM computation.

2. The loading distribution on the propeller blades is determined using the BEM and the average forces on the camber plane are calculated. Due to the non-uniform nature of the wake field, an unsteady BEM computation is required. From the forces on the camber plane at different blade positions a three-dimensional time-averaged force distribution can be constructed.

3. The time-averaged BEM propeller loading distribution is applied as a body force field in the RANS simulation. Therefore, the BEM force distribution has to be interpolated to the RANS grid. Several methods can be used to redistribute the forces, which are treated in more detail in Starke & Bosschers (2012). If necessary, the body forces are scaled to provide equal thrust in the RANS computation as determined by the boundary element method to correct for deficiencies in the interpolation procedure.

4. The total wake field is computed with RANS and the propeller induced velocities are subtracted to obtain the effective wake field. The induced velocities are determined from the BEM computation that provided the body forces and are time-averaged for the different blade positions.

5. The procedure is repeated from point 2 with the new effective wake field until convergence is reached, i.e. no change in thrust and effective wake velocities between consecutive RANS-BEM couplings.

An essential part of the coupling is the determination of the effective wake used for the BEM computations. Due to the presence of singularities at the collocation points of the BEM panels, determining the velocities close to or inside the propeller geometry, thus in the propeller plane, can result in numerical difficulties and lead to unrealistic velocity values. An alternative is to extract the induced velocities at a plane upstream of the propeller. However, earlier studies have shown that the effective wake accelerates towards the propeller plane and therefore strongly depends on the location of the extraction plane, as will be demonstrated later on. Different ways to determine the effective wake and the corresponding influence on propeller performance are discussed in detail in section 5.

3.2 Verification of the induced velocities

In order to have a consistent effective wake field, the body-force induced velocities in the RANS simulation should be identical to the induced velocities that follow from the BEM. Any deviation in induced velocities introduces an inconsistency in the effective wake. To evaluate the consistency of the induced velocities, an open water RANS-BEM coupling can be performed. In the open water simulation only the propeller is modelled, which is subjected to a uniform inflow.

Earlier studies have demonstrated that the induced velocities are sensitive to details in the the propeller modelling, which is different in the RANS and BEM simulations, see Starke & Bosschers (2012). For instance, in the RANS computations with body force distribution, the influence of the blade thickness on the flow is neglected. In the BEM the blade thickness is represented by the sources on the blades. To have consistent induced velocities the blade sources should not be taken into account for determining the BEM induced velocities. Furthermore a smooth force field in the RANS grid is required, which depends on the method that is used to interpolate the BEM loading distribution to the RANS grid.

The numerical set-up that is used in the open water computations is visualized in Figure 1. A cylindrical domain with uniform inflow prescribed at the inlet is used. At the exterior boundary a constant pressure is prescribed. The shaft extends from inlet to outlet with a free-slip boundary condition prescribed and the body forces representing the propeller action are applied in the middle of the domain. At the outlet an outflow boundary condition is set, which imposes a zero normal derivative of the flow variables.

An example of the flow field for a 5-bladed propeller at an advance ratio of $J = 0.924$ is shown in Figure 2. The acceleration of the flow behind the propeller is shown as well as the contraction of the wake. The mesh lines show the locations where a body force is applied in the RANS simulation. At $x/R = 0.3$ upstream of the propeller, represented by the black line in Figure 2, axial and radial induced velocities of the propeller for both ReFRESCO and PARNASSOS are compared to the PROCAL velocities in Figure 3. Similar induced velocities obtained from different RANS approaches are observed as well as a good agree-

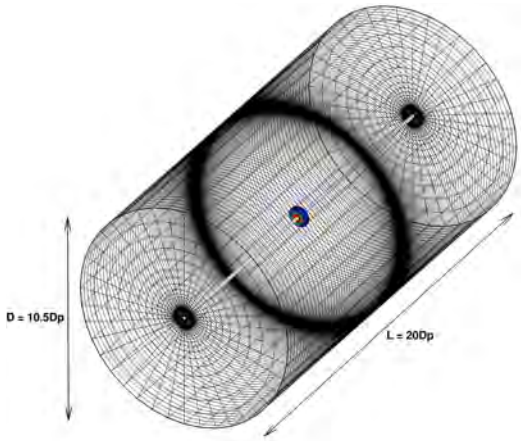

Figure 1: Domain for RANS-BEM open water computations with body forces.

ment between RANS and BEM. Overall the variation of induced velocities over the radial range is closely followed and both RANS codes show slightly higher axial induced velocities than the BEM.

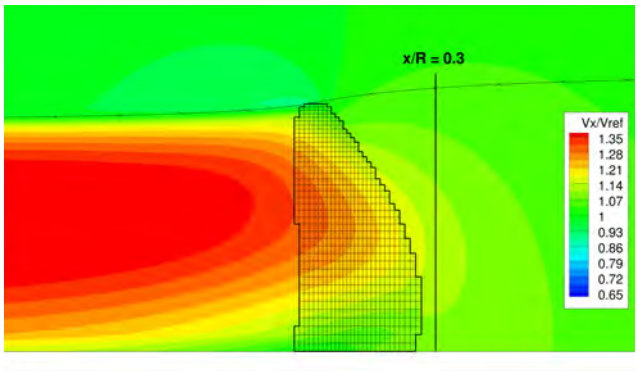

Figure 2: Axial velocity in RANS open water simulation.

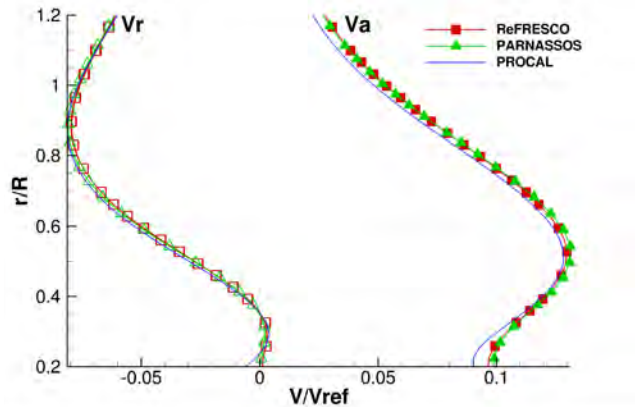

Figure 3: Comparison of induced velocities between RANS and BEM for propeller in open water. V_a (closed symbols) and V_r (open symbols) denote axial and radial induced velocities respectively.

In this study the results for one propeller geometry at a single advance ratio is given, but similar open water simulations were done for different operating conditions and propeller designs, see Starke & Bosschers (2012). These showed a similar agreement in induced velocities between RANS and BEM.

4 RANS-BEM RESULTS FOR THE KCS

The Kriso Container Ship (KCS) is a single-screw container ship that is often used in numerical studies, see for example Larsson et al. (2010). The particulars and operating conditions of this ship for model scale are listed in Table 1.

Table 1: Ship particulars and operating condition.

Length perpendiculars	L_{pp}	[m]	7.2785
Draught	T	[m]	0.342
Ship speed	V_s	[m/s]	2.196
Propeller diameter	D_p	[m]	0.25
Rotation rate	n	[rps]	9.5
Advance ratio	J		0.9246
Reynolds number	Re		$1.4 \cdot 10^7$
Froude number	Fn		0.26

For self-propulsion the propeller thrust equals the total resistance of the ship. Of the different resistance components, the wave resistance is related to the presence of a free surface. Because the determination of the free surface is often computationally intensive, an alternative is to perform a simulation with a flat fixed surface, a so called double-body approach. For self-propulsion, the wave resistance contribution has to be determined by other means, for example from other numerical methods or experiments and added to the double-body resistance. Depending on the operating condition, the presence of the free surface can also influence the flow field into the propeller. In this study results using both approaches will be presented, the ReFRESCO computations were performed using a double-body set-up and for PARNASSOS the free surface was included. Different grid set-ups were used in the PARNASSOS and ReFRESCO simulations. For both a block structured grid generation was applied that maintains geometric similarity for different sized grids.

4.1 Resistance and nominal wake field

In order to properly determine the interaction between propeller and hull, accurate predictions of both the ship's resistance and the wake field are essential. In this section the resistance prediction without propeller action is presented. The resulting nominal wake field provides a good initial condition for the RANS-BEM computations. Since the nominal wake field has some similarity to the effective wake field, it also provides a reference for the effective wake field.

An overview of the total resistance coefficient (C_T) and wake fraction (w) for different grid densities is given in Table 2, which are defined as:

$$C = \frac{R}{\frac{1}{2}\rho V_s^2 S} \tag{1}$$

$$1 - w = \frac{\int_{r_h}^{R_p} \left(\frac{v_a}{V_s}\right) r dr}{\int_{r_h}^{R_p} r dr} \tag{2}$$

where R represents the resistance, ρ the density, V_s the ship speed,S the wetted surface, r_h the hub radius, R_p the propeller radius and v_a the circumferentially averaged axial velocity. Because the ReFRESCO computations are done using a double-body set-up, an additional wave resistance component is added to the double-body drag to compare total resistance. The wave resistance component follows from the MARIN in-house non-linear potential method RAPID (Raven, 1996), resulting in $C_W = 0.51 \cdot 10^{-3}$ for the KCS in this service condition.

The largest resistance component at this Froude number is due to the frictional drag. The variation between consecutive finest grids is about 1% in total resistance for ReFRESCO. Compared to the experimental results a good agreement in total resistance is found for both PARNASSOS and ReFRESCO, slightly higher than the experimental value.

Table 2: Total resistance coefficient and wake fraction for KCS in nominal flow conditions for different grid densities. M denotes million of grid cells.

	$C_T \times 10^{-3}$	$1-w$
ReFRESCO		
3.3M	3.53	0.728
6.8M	3.56	0.724
14.4M	3.59	0.720
PARNASSOS		
0.8M	3.65	0.704
6.2M	3.64	0.720
Experimental. (Hino, 2005)	3.56	

The axial velocities of the nominal wake field for PARNASSOS and ReFRESCO are presented in Figure 4. The axial wake peak in the propeller top position (180°) is similar for both RANS codes. A slightly higher velocity in the top part of the disc at the outer radii is observed for PARNASSOS. Furthermore, a thicker boundary layer region is seen for the PARNASSOS results in the lower part of the propeller disc. The differences in wake field velocities are due to the presence of the free surface in the PARNASSOS computations as well as a different turbulence model and grid set-up for both codes. This variation in the ship's wake field will also affect the effective wake and therefore the propeller performance. The influence of the wake field for both approaches is shown in the next section.

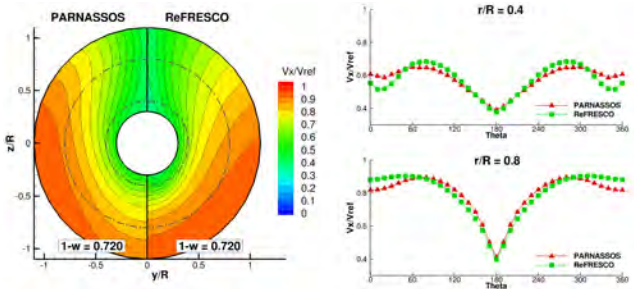

Figure 4: Axial velocities in the nominal wake field for PARNASSOS and ReFRESCO.

4.2 Self-propulsion

At the ship self propulsion point, the total resistance of the ship is balanced by the delivered thrust of the propeller. The required propeller thrust is obtained by adjusting the rotation rate of the propeller. The ship's resistance is extracted from the RANS computation and corrected for the additional towing force (skin friction correction due to higher viscous resistance at model scale than at full scale) and wave resistance if a double-body computation is performed.

For the KCS a RANS-BEM coupling was performed with both RANS codes and the resulting resistance and propeller characteristics are given in Table 3. The propeller thrust (K_T) and torque (K_Q) coefficients are defined as follows:

$$K_T = \frac{T}{\rho n^2 {D_p}^4}; K_Q = \frac{Q}{\rho n^2 {D_p}^5} \tag{3}$$

where T and Q denote the thrust and torque respectively. A similar variation in the resistance components and advance velocity between solutions on different ReFRESCO grids is seen as for the nominal case, in the order of 1% between finest consecutive grids for resistance and a smaller variation for the advance velocity. The total thrust value increases with grid refinement and tends to the experimental value. The total thrust in comparison with the experimental results deviates in the order of 1%. Only a small variation in rotation rate is seen for the different grids because the required thrust increases and average wake velocities decrease with increasing grid density. For PARNASSOS computations results on two grids are shown with a small variation in predicted rotation rate. Although a different numerical approach and set-up is used for both RANS codes, ReFRESCO and PARNASSOS show similar results in terms of resistance and propeller performance. Compared to the measurements a difference of 2 to 3% is seen for the rotation rate and required thrust. A larger difference in the order of 5 to 7% follows for the thrust and torque coefficient.

Table 3: KCS propeller performance characteristics for different grids compared with experimental results.

	T [N]	n [rps]	K_T	$10K_Q$
ReFRESCO				
3.3M	58.85	9.29	0.175	0.304
6.8M	59.65	9.31	0.176	0.306
14.4M	60.45	9.32	0.178	0.308
PARNASSOS				
0.8M	63.58	9.41	0.184	0.316
6.2M	61.59	9.39	0.179	0.310
Experimental (Larsson et al., 2010)	59.84	9.5	0.170	0.288

The axial velocities of the resulting effective wake fields for both codes are shown in Figure 5. The effective wake field and corresponding propeller performance are obtained here using extrapolation of the effective wake to the propeller plane. For reference the nominal wake field of the ReFRESCO simulation is also included. The difference between both RANS codes is similar for effective and nominal flow field, see also Figure 4. For the inner radii a closer agreement is seen in the effective field than in the nominal field. The effect of the different wake fields results in a higher rotation rate of about 1% for PARNASSOS compared to the ReFRESCO results.

Compared to the (ReFRESCO) nominal wake field, the effective field shows a lower wake peak with a similar velocity distribution at the outer radii and a smoother velocity distribution at the inner radii, where vorticity, and thus interaction effects, plays a larger role.

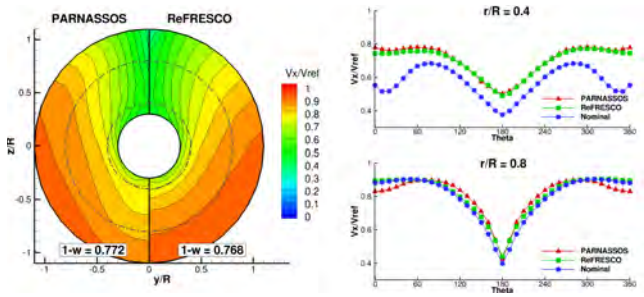

Figure 5: Comparison effective wake field KCS for PARNASSOS and ReFRESCO.

An integrated approach to study propeller-hull interaction allows to evaluate the effect of the propulsor on the hull and the wake field on the propeller loading distribution. Figure 6 shows the acceleration of the flow at the stern of the ship due to the propeller action. A large part of the flow is accelerated due to the propeller presence, but also regions of reversed flow are observed, located near the edges. At the tip and at the hull above the tip a flow reversal is observed due to the suction of the propeller, which influences the inflow to the propeller.

The propeller pressure distribution and time-averaged thrust distribution are presented in Figure 7. The non-uniform inflow produces the highest thrust in top position and a higher thrust on starboard side where the blade moves in downward direction (opposite to the transverse velocities).

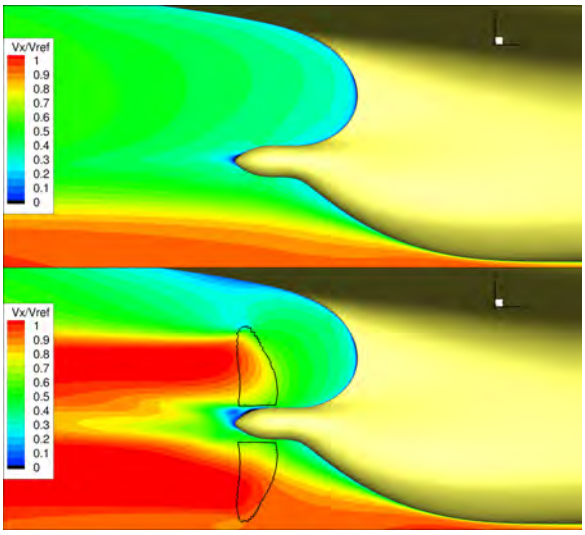

Figure 6: Axial velocity at the stern without (top) and with propeller action (bottom).

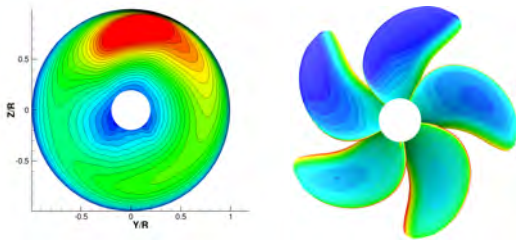

Figure 7: Thrust distribution (left) and blade pressure distribution on propeller back (right).

5 EFFECTIVE WAKE ANALYSIS

It is clear from Figure 6 that the (total) wake field upstream of the propeller is accelerating towards the propeller. For the effective wake this is not immediately obvious, since close to the propeller the total wake increases, but the induced velocities are also higher. If the effective wake has a negligible acceleration upstream of the propeller, the location where the effective wake is evaluated would not have a large influence. From the RANS-BEM computations it shows that also the effective wake is accelerating. This is visualized in Figure 8, in which the variation of the effective wake velocities in axial direction is presented. The values at $x/R = 0.0$ are the extrapolated effective wake velocities at the propeller plane.

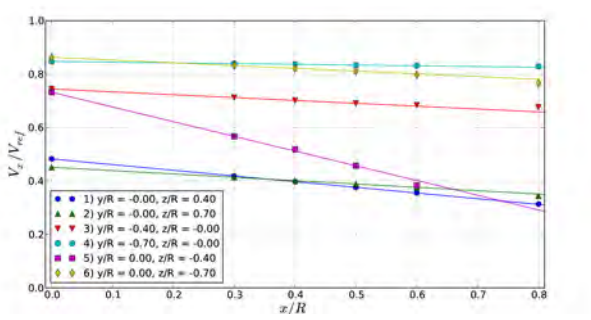

Figure 8: Variation of effective wake velocities with axial location for different points in the ship wake.

5.1 Determination of the effective wake

A logical choice for determining the effective wake would be the propeller reference plane. This plane is used to measure the nominal wake field in an experimental set-up, from which traditionally the effective wake field is derived. As mentioned earlier obtaining the induced velocities close to the propeller geometry leads to numerical difficulties for the BEM. To overcome this problem the following options are possible to determine an effective wake:

1. Determine the effective inflow in a straight plane upstream of the propeller, assuming that the acceleration of the effective wake is not significant.
2. Evaluate the effective inflow as close to the propeller as possible. For instance in a curved surface just ahead of the leading edge of the propeller blades.
3. Extrapolate the effective wake from two or more planes upstream of the propeller towards the propeller plane.

All these approaches can be found in the literature, but no clear relation has yet emerged between the type of approach and the accuracy of the results. The influence on the prediction of ship resistance and propeller performance of the listed options will be addressed in more detail. The different planes are visualized in Figure 9 which also shows the grid cells where the body forces are applied in the RANS simulation.
First the single straight planes upstream of the propeller are considered for a single grid to evaluate the influence of the effective wake acceleration on the propeller performance. The results are presented in Table 4 for PARNASSOS[1] and ReFRESCO, showing an influence in the order of 1% for propeller rotation rate between the different axial locations for both codes. This shows that the acceleration of the effective wake does influence the resulting propeller performance and indicates that for extrapolation an additional increase in rotation rate is expected.

[1]The (extrapolated) PARNASSOS values in Table 3 are slightly different than in Table 4. For the first the full ship geometry was taken into account, while for the latter only the starboard side was used.

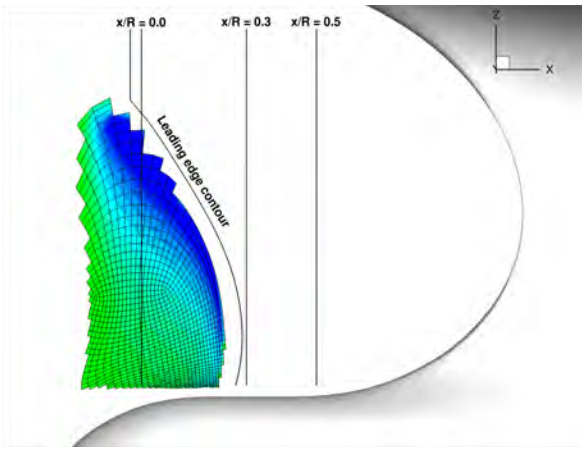

Figure 9: Location of different extrapolation planes at the stern. The contour represents the body force distribution in the RANS simulation.

When the velocities are extrapolated to the propeller reference plane, as presented in the results from the previous section, an additional increase in rotation rate is seen of about 2%. Due to higher axial flow velocities and the same required thrust, the propeller has to rotate faster in order to achieve this thrust. The planes used for the extrapolation are the $x/R = 0.5$ and $x/R = 0.3$ upstream planes for the ReFRESCO results and $x/R = 0.45$ and $x/R = 0.3$ for PARNASSOS. Figure 8 shows that for this case linear extrapolation seems justified for the axial velocities in most of the propeller disc, except in the lower part of the propeller disc. Although results of both RANS solvers are not the same, a similar influence is observed to the location of the plane where the effective wake is determined.

Table 4: KCS propeller performance characteristics for different extraction planes.

	T [N]	n [rps]	K_T	$10K_Q$
ReFRESCO (6.8M)				
x/R=0.50	59.72	9.02	0.188	0.322
x/R=0.40	59.71	9.08	0.186	0.319
x/R=0.30	59.71	9.14	0.183	0.314
Extrapolated	59.65	9.31	0.176	0.306
PARNASSOS (0.8M)				
x/R=0.45	60.88	9.11	0.188	0.323
x/R=0.30	60.87	9.22	0.184	0.316
Extrapolated	60.83	9.45	0.175	0.304

Another approach is to define a curved extraction plane that follows the leading edge contour of the propeller. This way the effective wake plane can be located as close to the body forces as possible, without resulting in numerical difficulties. An example of this type of extraction plane is visualized in Figure 9 with an offset of $x/R = 0.05$ from the

propeller leading edge. ReFRESCO results for the KCS are listed in Table 5. Multiple curved planes can also be used for extrapolation to the propeller reference plane. If linear extrapolation is justified a similar effective wake would be expected as for the extrapolation using straight planes. For the upper radii, a smaller extrapolation distance can be used, leading to a smaller extrapolation error.

Table 5: ReFRESCO (6.8M) propeller performance characteristics for a curved extraction plane that follows the leading edge (LE) contour.

	T [N]	n [rps]	K_T	$10K_Q$
LE Contour				
Single plane	59.65	9.24	0.179	0.311
Extrapolated	59.65	9.38	0.174	0.303

As expected a higher rotation rate is found for the single curved plane as for the straight plane, in the inner radii similar velocities as for the single (straight) plane at $x/R = 0.3$ are obtained, but higher velocities in the outer radii of the effective wake lead to an overall higher rotation rate. The results for the extrapolation with curved planes show a slightly higher rotation rate (within 1%) than for the extrapolation of the straight planes.
The influence on the effective wake velocities of plane location and shape is presented in Figure 10. At the lower radii the highest velocity are obtained for the extrapolated wake. The largest difference is observed at the lower side of the propeller disc.

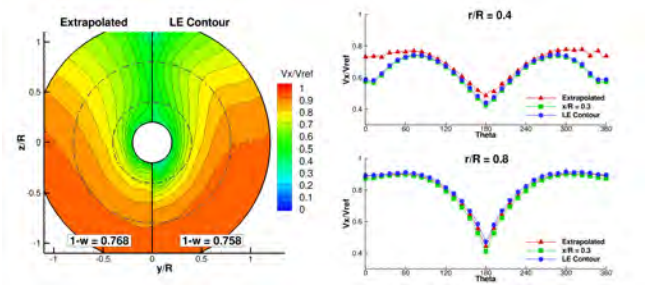

Figure 10: Comparison of effective wake field for extrapolated and single plane ($x/R = 0.3$ and LE Contour) approaches for ReFRESCO (6.8M).

The difference between using a single plane or extrapolation to the propeller plane is in the order of 2% when the single plane is chosen close to the propeller geometry. Extrapolation of the effective wake shows the best agreement with experimental values for both RANS solvers in terms of propeller rotation rate. Similar single screw vessels without upstream appendages also show the same trend. Although linear extrapolation seems justified for the single screw vessels treated here, difficulties can be expected when upstream devices are placed before the propeller, such as stators or pre-ducts. The presence of separation in the extrapolation planes is expected to introduce larger extrapolation errors in the effective wake field. Whether the extrapolation is still valid remains a topic of future work.

5.2 Comparison with NOMEFF

At MARIN the effective wake that serves as input for propeller design is normally obtained by correcting the nominal wake field with the force field method NOMEFF. A comparison between NOMEFF and ReFRESCO is presented in Figure 11, where the difference between the effective and nominal wake is shown. The NOMEFF effective field was obtained from the ReFRESCO nominal wake field for the $14.4M$ grid. For ReFRESCO the result for the extrapolated effective wake field is shown.

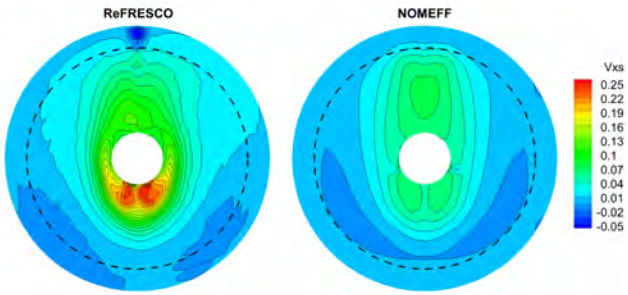

Figure 11: Difference in axial velocities between effective and nominal wake field for ReFRESCO (left) and NOMEFF (right). Dotted line indicates the propeller radius.

Both approaches show an increase of the axial velocities at the inner radii of the propeller disc and in the wake peak. In this region a thick boundary layer with high vorticity is present, which is affected by the propeller action. In the inner radii of the propeller disc a significantly higher velocity difference is observed for RANS-BEM than for NOMEFF. The largest difference between RANS-BEM and NOMEFF is observed in the lower part of the propeller disc close to the shaft. The location of the highest peak in the lower part of the disc seems to be identical in both approaches. Another interesting difference is in the top position at the outer radius, where a decreased axial velocity can be seen for the RANS-BEM. This is an effect that is not taken into account in the force-field method and is due to the region of decelerated flow above the propeller, also visualized in Figure 6.

Table 6: Propeller performance characteristics with NOMEFF effective wake field. The ReFRESCO (14.4M) nominal wake is used as input.

	T [N]	n [rps]	K_T	$10K_Q$
NOMEFF	60.45	9.19	0.183	0.315

The resulting propeller performance prediction when using

the NOMEFF effective wake field as input for the BEM is listed in Table 6. The prediction of rotation rate and corresponding thrust and torque coefficients is similar as when determining the effective wake using a single plane upstream and thus slightly lower than the extrapolated wake results.

6 CONCLUDING REMARKS

In this study a numerical approach to investigate propeller-hull interaction has been applied by coupling two different RANS solvers for the hull flow with a BEM model for the propeller, resulting in the following conclusions:

- Results for the RANS-BEM coupling for a single-screw container ship (KCS) show a prediction of the rotation rate and propeller thrust within 2 to 3% of the experimental values on the finest grid. Different RANS approaches with and without the free surface show an influence on the effective wake leading to differences in prediction of rotation rate of about 1%.
- The essential part of the RANS-BEM coupling remains how and where to determine the effective wake field. It was demonstrated that the effective wake accelerates towards the propeller. Extrapolation of the effective wake in downstream direction towards the propeller reference plane leads to a further increase of the axial velocity which results in an increase of 2 to 3% in rotation rate compared to using a plane upstream of the propeller.
- Comparison of the effective wake field obtained from the RANS-BEM results with the MARIN force-field method NOMEFF shows some significant differences, especially at the inner radii in the lower part of the propeller disc, where a higher axial velocity in the wake field of the RANS-BEM coupling is observed. The higher wake velocities result in a higher rotation rate for the RANS-BEM simulations. In this case RANS-BEM with extrapolation of the wake field shows a better agreement with the experimental results in terms of propeller performance than NOMEFF.

REFERENCES

Bosschers, J., Vaz, G., Starke, A. R. & van Wijngaarden, E., 2008. 'Computational analysis of propeller sheet cavitation and propeller-ship interaction'. In Proceedings of RINA conference MARINE CFD2008. Southampton, UK.

Carlton, J. S., 2007. Marine propellers and propulsion. Butterworth-Heinemann Ltd.

Dacles-Mariani, J., Zilliac, G. G., Chow, J. S. & Bradshaw, P., 1995. 'Numerical/experimental study of a wingtip vortex in the near field'. AIAA Journal, **33**, pp. 1561–1568.

Hino, T. (ed.), 2005. CFD workshop Tokyo.

Hoekstra, M., 1999. Numerical simulation of ship stern flows with a space-marching Navier-Stokes method. Ph.D. thesis, Delft University of Technology.

Hoekstra, M. & Vaz, G., 2009. 'The partial cavity on a 2D foil revisited'. In Proceedings of Cav2009 Conference. Ann Harbour, Michigan, USA.

Larsson, L., Stern, F. & Visonneau, M. (eds.), 2010. Gothenburg 2010, A workshop on numerical ship hydrodynamics, vol. II.

Menter, F., 1997. 'Eddy-viscosity transport equations and their relation to the k-e model'. Journal of Fluids Engineering, **119**, pp. 876–884.

Van der Ploeg, A., Eça, L. & Hoekstra, M., 2000. 'Combining accuracy and efficiency with robustness in ship stern flow calculation'. 23rd Symp. Naval Hydrodynamics. Val de Rueil, France.

Raven, H. C., 1996. A solution method for the nonlinear ship wave resistance problem. Ph.D. thesis, Delft University of Technology.

Raven, H. C., Van der Ploeg, A. & Starke, A. R., 2004. 'Computation of free-surface viscous flows at model and full-scale by a steady iterative approach'. 25th Symp. Naval Hydrodynamics. St. John's, Canada.

Rijpkema, D. & Vaz, G., 2011. 'Viscous flow computations on propulsors: verification, validation and scale effects'. Developments in Marine CFD. RINA, London, UK.

Starke, A. R. & Bosschers, J., 2012. 'Analysis of scale effects in ship powering performance using a hybrid RANS-BEM approach'. 29th Symp. Naval Hydrodynamics. Gothenburg, Sweden.

Van Brummelen, E. H., Raven, H. C. & Koren, B., 2001. 'Efficient numerical solution of steady free-surface Navier-Stokes flow'. Jnl. Computational Physics, **174**, pp. 120–137.

Van Gent, W., 1986. 'A model for propeller-ship wake interaction'. In Proceedings of ISPC. Wuxi, China.

Vaz, G. & Bosschers, J., 2006. 'Modelling of three dimensional sheet cavitation on marine propellers using a boundary element method'. In Proceedings of 6th Int. Symp. on Cavitation CAV2006. Wageningen, The Netherlands.

Vaz, G., Toxopeus, S. L. & Holmes, S., 2010. 'Calculation of manoeuvring forces on submarines using two viscous-flow solvers'. In Proceedings of OMAE2010. Shanghai, China.